Virology 462-463 (2014) 309–317

Contents lists available at ScienceDirect

Virology

journal homepage: www.elsevier.com/locate/yviro

Lineage diversification of pigeon paramyxovirus effect re-emergence potential in chickens

Yee Ling Chong [a,b,*], Oekyung Kim [a], Mary Poss [a,*]

[a] Center for Infectious Disease Dynamics, Department of Biology, The Pennsylvania State University, University Park, PA 16802, USA
[b] Department of Zoology, Faculty of Resource Science and Technology, Universiti Malaysia Sarawak, 94300 Kota Samarahan, Sarawak, Malaysia

ARTICLE INFO

Article history:
Received 11 February 2014
Returned to author for revisions
8 June 2014
Accepted 9 June 2014
Available online 8 July 2014

Keywords:
Paramyxovirus
Genetic-phenotypic association
Multivariate analysis

ABSTRACT

Genotype VI-paramyxovirus (GVI-PMV1) is a major cause of epidemic Newcastle-like disease in Columbiformes. This genotype of avian paramyxovirus type 1 has diversified rapidly since its introduction into the US in 1982 resulting in two extant lineages, which have different population growth properties. Although some GVI-PMV1s replicate poorly in chickens, it is possible that variants with different replicative or pathogenic potential in chickens exist among the genetically-diverse GVI-PMV1s strains. To determine if variants of Columbiform GVI-PMV1 with different phylogenetic affiliations have distinct phenotypic properties in chickens, we investigated the replicative properties of 10 naturally circulating pigeon-derived isolates representing four subgroups of GVI-PMV1 in primary chicken lung epithelial cells and in chicken embryos. Our data demonstrate that GVI-PMV1 variants have different infection phenotypes in their chicken source host and that properties reflect subgroup affiliation. These subgroup replicative properties are consistent with observed dynamics of viral population growth.

Introduction

Genotype-VI paramyxovirus (GVI-PMV1) arose from cross-species transmissions from chickens to pigeons and now has strong host fidelity to pigeons (Chong et al., 2013). GVI-PMV1 strains cause systemic infection in pigeons resulting in respiratory disease (Toro et al., 2005) and with notable symptoms in the central nervous system and gastrointestinal tract (Barber et al., 2010). GVI-PMV1 is most frequently detected in Columbiformes (*i.e.* pigeons and doves) populations (Kim et al., 2008) but continues to cause sporadic outbreaks in chickens (Abolnik et al., 2008; Hassan et al., 2010; Pedersen et al., 2004). Despite possessing the genetic signature for virulence at the F gene cleavage site, GVI-PMV1 isolates typically replicate poorly and are not virulent in chickens in experimental studies (Meulemans et al., 2002). The virulence potential of GVI-PMV1 in chickens is determined by virus strain as well as by the age of chickens, route and intensity of viral inoculations used in the experimental settings (Gelb et al., 1987; King, 1996; Pearson et al., 1987; Toro et al., 2005). For example, the consequences of infection by different GVI-PMV1 strains range from mild respiratory disease to neurotropic disease and mortality in experimentally infected chickens (Gelb et al., 1987; Pearson et al., 1987; Toro et al., 2005). Serial passage in chickens or embryonated eggs increased virulence (Dortmans et al., 2011; Fuller et al., 2007; Kommers et al., 2001) and enhanced the replication of GVI-PMV1 (Dortmans et al., 2011), and in one study isolates recovered from experimentally passaged virus in chickens had only three mutations in two viral genes, P and L (Dortmans et al., 2011). This data suggest that small changes in the viral genome are sufficient to allow GVI-PMV1 infections in chickens.

After the emergence of GVI-PMV1 in European Columbiformes in the 1980s, there were at least three virus introductions to North America. GVI-PMV1 in North American Columbiformes has evolved at a high substitution rate and there is measurable genetic diversity in contemporary strains (Chong et al., 2013). Two extant lineages, GVIbii-*d* and -*g*, have diversified locally; the former has maintained a fairly constant viral population size over time, whereas the later has experienced exponential population growth (Chong et al., 2013). Despite the apparent fidelity of GVI-PMV1 for pigeons, outbreaks in poultry continue to be reported in many countries (Abolnik et al., 2008; Hassan et al., 2010; Mase et al., 2002; Pedersen et al., 2004; Ujvari et al., 2003) and GVI-PMV1 can be isolated from chickens in the absence of an epizootic. It is therefore of substantial interest for both risk assessment and diagnostics to determine if the genetic diversification of the GVIbii-*d* and -*g* lineages derived from the pigeons has

* Corresponding authors.
E-mail addresses: yeelingchong@gmail.com (Y.L. Chong), mposs@bx.psu.edu (M. Poss).

http://dx.doi.org/10.1016/j.virol.2014.06.007
0042-6822/

conferred unique infection phenotypes in chickens, and whether phenotypic properties in chickens are associated with the observed viral population growth patterns that characterize each lineage.

To this end, we assessed the organismal and cellular replication of 10 GVI-PMV1 isolates representing GVIbii-*d* and -*g* lineages obtained from naturally infected pigeons. The complete genomes of these selected isolates were sequenced. Linear discriminant analyses (LDA) were used to determine if infection phenotype correlated with viral genotype. Our data indicate that rapid diversification of a virus in a new host has consequences to infection properties in the original host. Data linking genotype and phenotype of viruses adapting to new hosts is of substantial importance as many important virus infections in humans and animals arise from cross-species transmission.

Results

Evolutionary history of GVI-PMV1 isolates used in this study

Ten GVI-PMV1 isolates obtained from sick pigeons submitted to the Animal Diagnostic Lab were selected based on the phylogenetic affiliations of the F gene (Fig. 1A), and were assigned to subgroups A – D based on bootstrap support. Subgroup A – C are GVIbii-*g* viruses, which are undergoing population expansion, while subgroup D is a member of lineage GVIbii-*d*, which demonstrates constant population size (Fig. 1A, upper inset).

We estimated recombination and selection profiles on these 10 isolates in relation to 51 isolates that were previously described (Chong et al., 2013) (Fig. S1). The phylogenetic affiliations of all isolates were consistent based F (Fig. 1), P, HN and on concatenated genes (Fig. S1), indicating that there was no recombination in this region of the genome (Chong et al., 2010). Using codon-based models and maximum likelihood methods implemented in PAML (Yang, 1997) and the Datamonkey webserver (Pond and Frost, 2005), we demonstrated that the overall d_N/d_S of each of the three genes was less than 1 indicating that purifying selection was predominant. Four codons in the P protein and one codon in F protein were under positive selection (Fig. 1B). Two of the four positively selected codons (*i.e.* 77 and 92) in P were predicted phosphorylation sites and fall in the region of P that overlaps with the small V protein, which is produced by post-transcriptional editing (Steward et al., 1993) (Table S3). In contrast, none of the codons in HN were under positive selection.

Survival kinetics of 10-day old chicken embryos infected with ten GVI-PMV1 isolates

We assessed the relative pathogenic potential of each isolate in ten-day old chicken embryos inoculated *via* the allantoic fluid route by recording the number of embryos that died every 12 h for seven days. The survival rates of chicken embryos infected with each virus differed ($P < 0.001$; Cox proportional hazards regression model), and were partially correlated with their subgroup classification (Fig. 2A). All embryos inoculated with subgroup A, B, and D viruses succumbed to infection within the experiment periods. PA-0725 (the only B subgroup virus) killed all embryos by 114 hpi, which was similar to that observed for the vaccine strain LaSota. The time to death of embryos infected with A and D subgroups ranged from 122–144 hpi. In contrast, embryos inoculated with subgroup C viruses had the longest survival times and there was no embryo mortality associated with na-106 inoculation.

Systemic infection in 18-day old chicken embryos

Chicken embryos have multiple tissues to support virus infection and each is capable of mounting a distinct host innate defense. Embryos are therefore reasonable surrogates for *in vivo* infection. As the 10 isolates of pigeon GVI-PMV1 showed different effects in chicken embryos at early [10–12 days] developmental stages, we further evaluated each virus for the ability to replicate in lung, liver, and spleen of chicken embryos at later developmental stages [18–20 days]. After 48 hpi, all embryos were alive and there were no gross pathological alterations of internal organs.

Viral transcripts from all 10 GVIb viruses and LaSota were detected in both lung and liver tissues. Moreover, all viruses except for PA-0725 and PA-0704 showed higher viral transcripts productions in lung, which is the primary site of infection following amniotic inoculation, compared to liver ($P < 0.05$). Although there were significant differences among the viruses in viral transcript production in lung (i.e production of both MD-0719 and PA-0805 transcripts in lung was significantly higher than na-0106 and PA-0810 ($P < 0.05$)) there was no apparent correlation between transcript production and virus subgroup. However, there were significant effects of both tissue type and virus subgroup on the total viral transcript production ($P < 0.05$; factorial ANOVA test) (Fig. 2B). In liver, PA-0725 (B subgroup) produced a higher level of viral transcripts than na-0101 and PA-0712 (D subgroup), na-0106 and NJ-0717 (C subgroup), and NJ-0607 (A subgroup) [$P \leq 0.01$]. Further, detection of viral transcripts in spleen is indicative of systemic infection. Only PA-0725 consistently dispersed to spleen; PA-0704 and NY-0717 transcripts were each found in spleen in one of seven replicates. While other GVI-PMV1 viruses and the low pathogenic LaSota vaccine strain were able to disseminate to liver, they failed to spread into spleens of the infected embryos within 48 hpi (Fig. 2B). The ability of PA-0725 to disseminate from the site of inoculation and produce the highest levels of viral transcripts may be related to the shorter survival time of embryos infected with PA-0725.

GVI-PMV1 infection in chicken primary lung epithelial cells

The *in ovo* data demonstrated that there was variation in the replication capacities of the 10 GVI-PMV1 isolates in chicken embryo tissues. We further evaluated replication properties *in vitro* using primary chicken lung epithelial cells. The production of cell-free viral RNA (detected by qRT-PCR) and infectious viral particles (detected by $TCID_{50}$ assay) differed among the 10 GVI-PMV1 viruses at early time points ($P < 0.0001$, ANCOVA; Fig. 3 and S2). At 12 hpi, viral RNA and infectious viral particles were detectable in supernatant of all cultures, with PA-0725 producing the highest amounts. Three viruses from subgroups C and D (PA-0805, na-0101 and PA-0712) had the lowest total amount of cell-free viral RNA at 12 hpi (below 10^8 total viral RNA/ml) but these three viruses had the fastest rate of viral RNA production between 12 and 20 hpi. By 36 hpi all viruses except na-0101 and LaSota had comparable amounts of viral RNA ($\sim 10^{10}$ total viral RNA/ml). All viruses had between 1 and 2 $\log_{10}$ fewer infectious particles than total viral RNA in the supernatant at each measured time point (Fig. S1).

Type I IFN induction by GVI-PMV1 in infected chicken primary lung epithelial cells

Host cells make and release type I interferon (IFN) in response to virus infection. Type I IFNs, also called IFN-α/β, possess pleiotropic capabilities that modulate innate and adaptive immune responses, cell growth, and apoptosis (Goodbourn et al., 2000) and inhibit virus replication. We measured IFN β transcript levels in

A

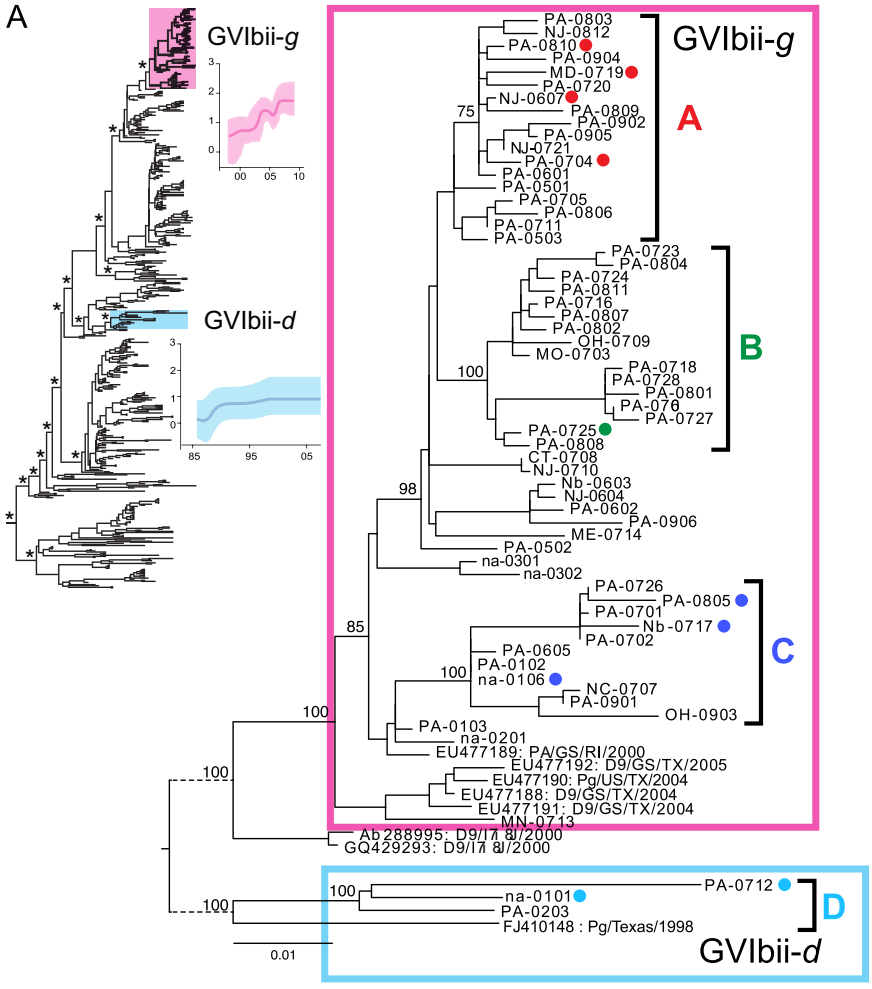

B

Isolates	Subgroup	P				F
		47	77	89	92	10
PA-0810	A	L	L	L	S	L
MD-0719		L	L	L	S	L
NJ-0607		L	L	L	S	L
PA-0704		L	L	L	S	L
PA-0725	B	L	F	L	S	L
PA-0805	C	L	S	L	P	L
Nb-0717		L	S	L	T	L
na-0106		L	S	L	P	L
na-0101	D	P	S	P	P	L
PA-0712		P	S	P	P	P

Fig. 1. Classification of GVI-PMV1 isolates based on lineage clustering in the phylogeny and selective pressure analysis. (A: Left Panel) Bayesian phylogeny of GVIb-PMV1 F gene. Posterior probability values of 0.75 or greater are shown as asterisk adjacent to the selected tree nodes. Two graph insets show the Bayesian skyline plots that illustrate the changes in virus population dynamics over time of the two GVIbii-PMV1 North American lineages, GVIbii-*d* ($n=17$; 1987–2007) and GVIbii-*g* ($n=76$; 2000–2009); the shaded red and blue bands give the 95% HPD intervals of the estimates for GVIbii-*d* and -*g* respectively. Both the Bayesian tree and skyline plots were adapted from Chong et al. (2013), Figs. 1 and 3. (A: Right Panel) 10 isolates indicated by colored dots after the strain names in the phylogeny are those selected for phenotypic characterizations and grouped into subgroups A (red), B (green), C (blue), and D (cyan) (sequence information at Table S3). Bootstrap supports for major lineages are shown. The branch length scale has a unit of substitutions/site. The long branches between GVIbii-*g* and -*d* are not to scale and indicated as in dashed lines. (B) The table shows the amino acid signatures in five positively selected sites for the 10 virus strains grouped in their respective subgroups (A–D). P represents the shared P/V co-amino terminal region and F represents the F protein. Gray boxes highlight the potential phosphorylation sites for selected isolates at 77 and 92 residues in P/V. Amino acid designation is given as single letter code, L=leucine, S=serine, T=threonine, F=phenylalanine, P=proline.

response to infection with the 10 GVI_PMV1 isolates over 16 h of infection to determine if expression of this cytokine correlated with differences in virus subgroup or replication profile. Our data show that both virus subgroup and infection time have significant effects on chicken IFN β transcript production ($P<0.05$; factorial ANOVA tests) (Fig. 4). At 6 h of infection, there were no significant

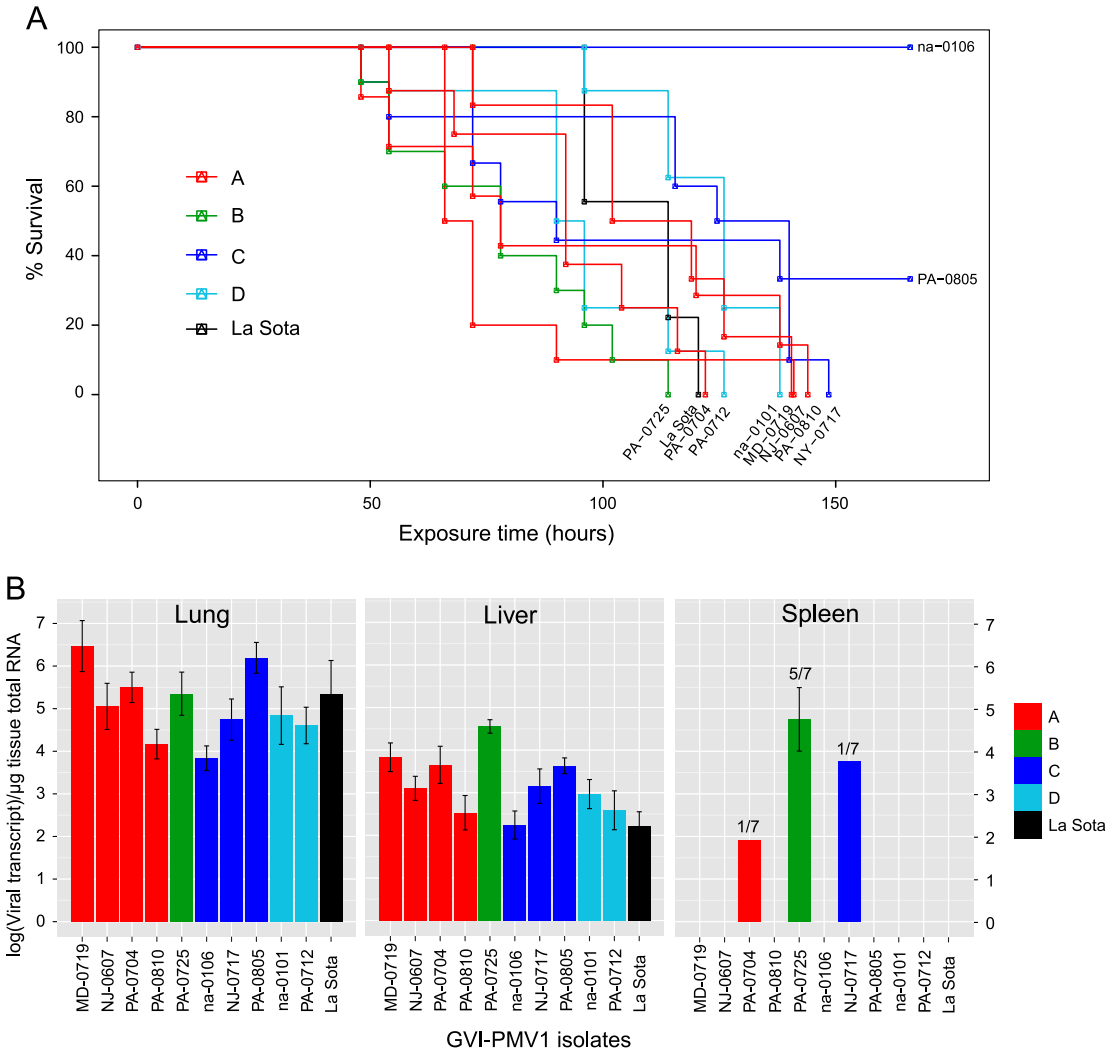

Fig. 2. *In ovo* experiments: (A) Chicken embryos survival and (B) GVI-PMV1 dissemination. (A) Survival of 10-day old chicken embryos infected with GVI-PMV1 isolates based on Kaplan – Meier curve. Vertical and horizontal scales depict the percentage of surviving embryos at each time (hours post-infection), respectively. The log-rank test of survival trend was significant for comparison between infected virus subgroups ($P<0.001$) based on both Efron approximation and Breslow methods. A–D indicate four virus subgroups shown in Fig. 1. LaSota vaccine strain, which replicates efficiently in chicken but does not cause systemic infection (Wakamatsu et al., 2006) was included for reference. PBS-sham inoculation was included as a negative control. All embryos survived until the end of experiment. (B) GVI-PMV1 dissemination in different tissues of 18-day old infected chicken embryos at 48 hpi. Data show the normalized level of cell-associated virus transcript determined by qRT-PCR. Error bars indicate ± standard errors. No viral transcripts were detected in PBS-sham inoculated specimens. The color bars A (red), B (green), C (blue), and D (cyan) indicate classification based on phylogenetic subgroup; while the black bar indicates LaSota GII vaccine strain. Virus name is indicated on the horizontal axis. Viral transcripts from all viruses were detected in both lung and liver tissues. Note that in spleen, there are no error bars for NY-0717 and PA-0704 because estimates of virus transcript number were based on a single positive sample (*i.e.* the inset shows the number of embryos assessed and the number with detectable transcripts for spleen tissues). The viruses, tissues and the interaction effects were significantly different based on the viral transcripts (factorial ANOVA, $P<1\times10^{-6}$).

differences in IFN β expression levels from cells infected with any virus as compared to PBS-sham control, except for a slight increase in expression induced by NY-0717 ($P=0.051$ two-sample *t*-test). Subgroup D viruses, which have a stable population growth profile (Fig. 1A), induced higher IFN expression compared to other viral subgroups although timing and magnitude of IFN induction varied among isolates. Specifically, IFN expression was elevated in cells infected with PA-0712 at 10 h exposure time while na-0101 infected cells had 102-fold increase in IFN expression compared to PBS-sham control at 16 h post-infection. Of interest, subgroup D viruses also had lower levels of virus production at 12 h (Fig. 3). This inverse association between virus production and IFN was not apparent with other viruses. In particular, PA-0725 (subgroup B), which is capable of systemic spread, had high levels of viral replication and demonstrated a 5-fold increase in IFN expression at 14 and 16 h exposure times.

Multivariate analyses of phenotype properties and GVI-PMV1 subgroup

We employed multivariate statistical analyses to determine the association of aggregate phenotype properties with viral subgroup affiliation; analyses of *in vitro* and *in ovo* infection data were done separately because of different biological experimental settings. *in vitro* phenotype parameters include: cell-free viral RNA production at four time points (designated as REP12, REP20, REP28, REP36); infectious viral particles at four time points (designated as TCID12, TCID20, TCID28, TCID36); and IFN β transcript production at four exposure times (designated as IFN6, IFN10, IFN14, IFN16). *In ovo* phenotype parameters include: cell-associated viral transcript levels in lung, liver, and spleen of 18-day old embryos and time (in hours) to kill 100% of 10-day old embryos (designated as DT100). We recorded the death time as 180 h for embryos that

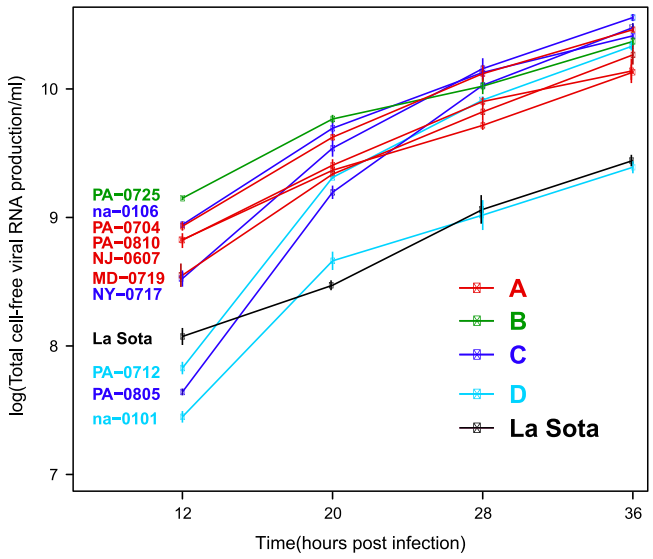

Fig. 3. GVI-PMV1 replication kinetics on chicken lung primary epithelial cells. The total cell-free viral RNA production was enumerated based on qRT-PCR and is represented as log total cell-tree viral RNA production per ml tissue culture supernatant. Error bars indicate the ± standard errors. A–D indicate four virus subgroups, using the same color scheme as in Fig. 2. Time in hours is indicated on the *x* axis. See Fig S2 for data on infectious virus production based on TCID50 assays.

survived throughout the experimental observation period. Our composite phenotype properties from both *in vitro* and *in ovo* systems differ significantly across GVI-PMV1 subgroups ($P < 0.00001$; MANOVA Pillai's trace test).

Discriminate analysis of phenotype properties and virus subgroups

Our primary research question was whether the divergent viral genotypes that have arisen in the US since the introduction of GVIb have different replicative properties in the original chicken host. To address this question we first used an unsupervised principal component analysis (PCA) to investigate patterns in our multi-dimensional data. The variance explained by linear combination of phenotype properties in PCA based on either *in vitro* or *in ovo* data did not group the viruses into their respective subgroups (data not shown). Hence, we applied linear discriminant analysis (LDA) to identify linear combinations of variables that best separate the viruses among their subgroups.

The 12 phenotypic properties from *in vitro* data (full model) were able to separate the viruses according to their phylogenetic subgroups (Fig. 5A) based on the feature loadings from the LDA bi-plot. In the first linear discriminant axis (LD1, 56.3% of trace), IFN10 and REP12 played a prominent role in separating GVIbii-*d* viruses (subgroup D) from GVIbii-*g* viruses (subgroups A, B, and C). The second LD axis (LD2, 25.8% of the trace) separated viruses in

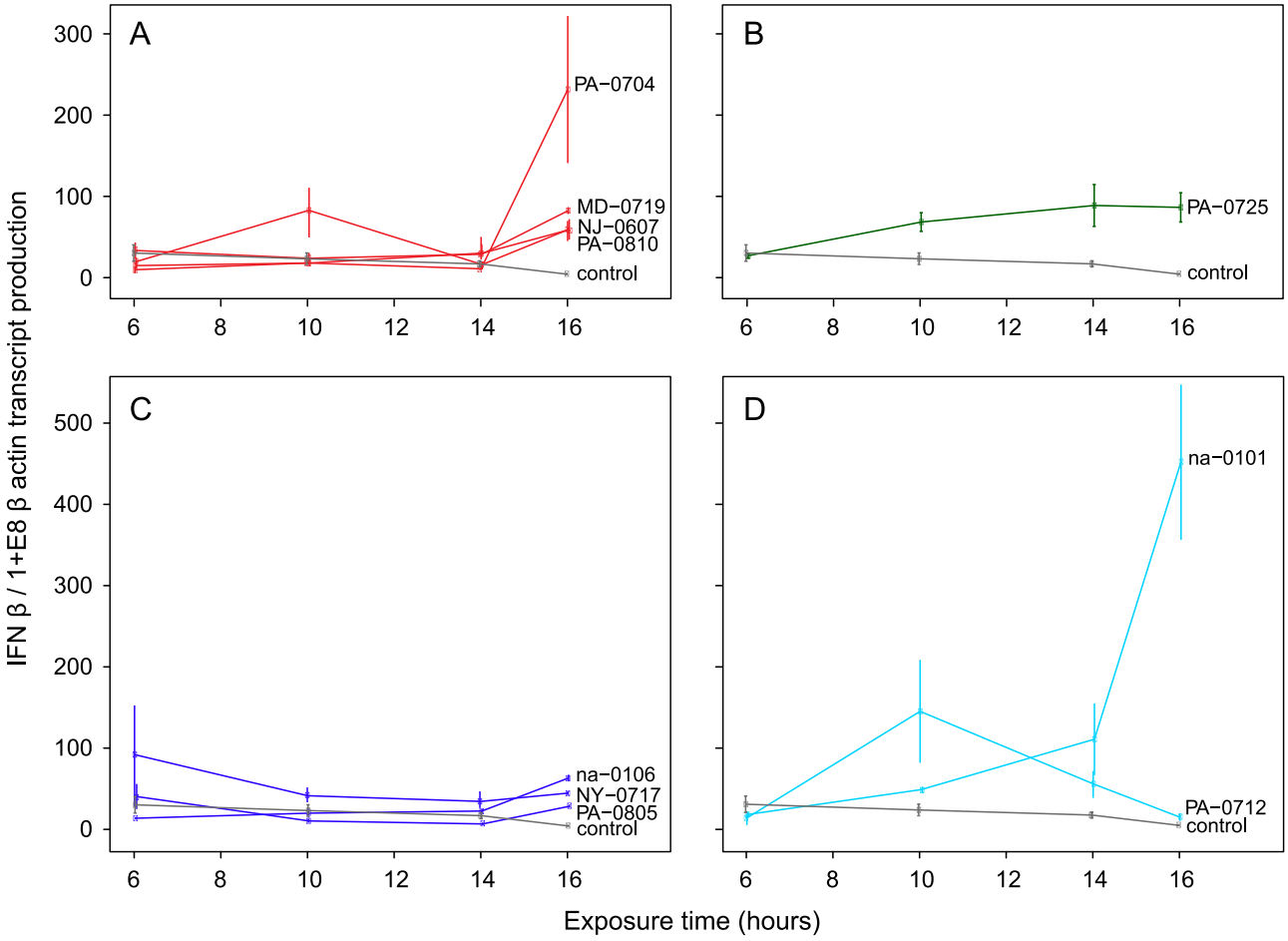

Fig. 4. Chicken IFN β expression by GVI-PMV1 infection at different exposure times. The IFN β and β-actin transcripts were enumerated based on qRT-PCR. Data are displayed as the ration of IFN β transcript number per 1×10^8 β actin transcripts. Error bars indicate the ± standard error (± se). Panel A–D indicate the classification based on virus subgroups A–D. The color scheme is as shown in Fig. 2. Time post-infection is shown on the *x* axis.

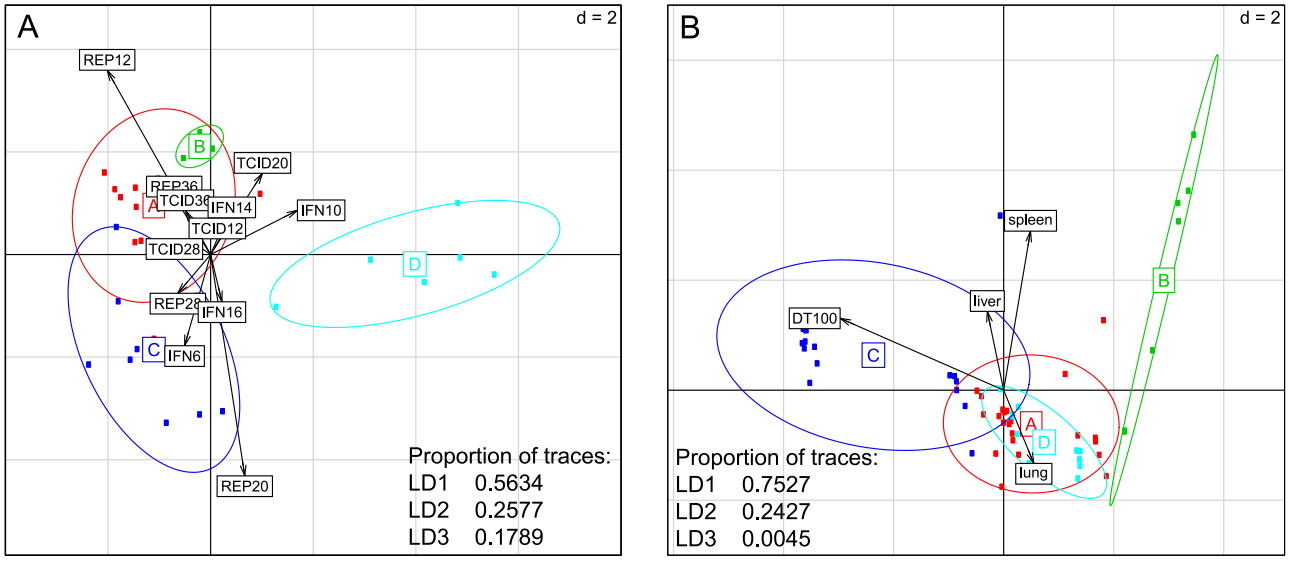

Fig. 5. LDA bi-plot based on phenotypic parameters from *in vitro* and *in ovo* studies. Panel A indicates the bi-plot generated by fitting the full model of 12 parameters determined from *in vitro* studies. The arrows illustrate loadings of 12 response variables, related to production of total viral RNA at different post-infection time points [REP12, REP20, REP28, REP36], infectious viral particles at different post-infection time points [TCID12, TCID20, TCID28, TCID36] and IFN transcript levels at different exposure times [IFN6, IFN10, IFN14, and IFN16] viral transcripts as described in Section 4. Each arrow and its orientation indicate the role of each phenotypic parameter in relation to the LDA directions. The virus subgroups are represented by different colors scheme as shown in Fig. 2. Elliptical contours captured the positive coefficient variability of each group with their data points in the plane. The insets indicate the proportion of traces (summed to 1) explained by the LD directions. Panel B represents the bi-plot generated by a fitting model based on the four parameters [time for 100% embryo lethal effect time (DT100)], viral transcript level in embryos tissues (lung, liver and spleen) in *in ovo* studies. The explanation of length and orientation of arrows, and the elliptical contours is described in panel A.

subgroup A and B from those in the C subgroup, driven primarily by opposing contributions of REP12 and REP20.

Because viral replication at early times of infection significantly contributed to the subgroup separation using all 12 *in vitro* parameters, we evaluated several reduced LDA models to determine if similar subgroup discriminant patterns could be recovered with equivalent contrasts weights and proportion of traces. Subgroup resolution was comparable to the full model if the later time points for cell-free viral RNA and infectious virus particles were omitted (Panel A; Fig. S3). Models based on cell-free viral RNA levels (Panel B; Fig. S3), infectious particles production (Panel C; Fig. S3) or IFNβ transcript abundance (Panel D; Fig. S3) alone did not resolve viral subgroups.

LDA was also performed to identify combinations of *in ovo* phenotype properties that discriminate among the four virus subgroups. B is well separated from C subgroup, contributed mainly by loading values of viral transcript levels in lung and spleen, as well as embryo lethal effect time (DT100) (Fig. 5B). A and D subgroups were not resolved. Without the embryo death time (DT100) parameter, A, C and D subgroups collapsed (Fig. S4).

Discussion

Our previous data showed that GVI-PMV1 viruses established in Columbiforme populations *via* successful cross-species transmission events from chickens about three decades ago (Chong et al., 2013). In North America, GVIbii-PMV1 arose from multiple introduction events leading to the emergence of genetic lineages with different population growth patterns (Fig. 1A). In the present study, we investigated the consequences of viral diversification in the new host (*i.e.* pigeons) on the replication properties in the source host (*i.e.* chickens). In order to gain insights into the association of GVI lineage and subgroup affiliation and phenotype, we evaluated the replication of pigeon-derived GVI isolates in both cellular and organismal chicken systems.

The 10 GVI-PMV1 isolates used in this study would be considered lentogenic strains based on embryo death time (Liu et al., 2006), which is similar to that of the vaccine strain LaSota. Nevertheless, the ability of GVI viruses to kill 10-day chicken embryos varied and correlated with replication properties in older embryos. The survival curves for 10-day embryos infected with PA-0725 (subgroup B) were shorter than for the other viruses, and PA-0725 disseminated to the spleen and produced the highest level of viral transcripts in the liver of 19-day embryos. The correlation of GVI-PMV1 viral replication with systemic spread in infected chickens has been previously noted (Dortmans et al., 2010).

The type I IFN response, which is an integral part of the host innate immune response, is a first line of cellular defense against virus infections (Goodbourn et al., 2000). IFN β elicits expression of downstream genes that restrict viral replication in infected and uninfected cells (van Boxel-Dezaire et al., 2006; Wesoly et al., 2007). Here we show that the four subgroups of GVI-PMV1 viruses evaluated induce different patterns of IFN expression and have different replication properties *in vitro*. An inverse relationship of virus production and interferon expression level is expected if there is an effective anti-viral response or effective viral antagonism of that response. If the host anti-viral response is effective, induction of IFN β should correlate with decreased replication efficiency. This pattern was observed for D subgroup viruses (lineage GVIbii-*d*) and distinguishes them from the three virus subgroups of GVIbii-*g* in the LDA (Fig. 5A). A second expected scenario is viruses that do not induce or actively antagonize IFN β early in infection will have higher virus production, which we observed in subgroups A and C viruses (Fig. 5A). Interestingly, these *in vitro* properties observed in chicken cells correlate with the differences in lineage population dynamics in pigeons (Fig. 1A). D subgroup viruses have maintained constant population size in pigeons over the last two decades and in our studies, they induce higher IFN β levels and have lower viral replication efficiency in chickens. In contrast, subgroup A and C viruses, which are from lineage GVI-*g*, show exponential growth in pigeons, and are poor inducers of IFN in chickens. We are aware that the observed

separation between GVIbii-*d* and GVIbii-*g* viruses based on LDA may be affected by the small samples of each subgroup. However, this multivariate data indicate possible subgroup specific phenotypic properties of GVI-PMV1 viruses from North America.

An intriguing third scenario is that there is direct correlation between IFN induction and virus production, which we observed for PA-0725 (subgroup B) infection. Paramyxoviruses (including PMV1) encode V proteins that block various components of IFN pathways (Childs et al., 2007; Childs et al., 2009; Huang et al., 2003; Mebatsion et al., 2001; Park et al., 2003; Poole et al., 2002), either by targeting the cellular helicase MDA-5 at an early step of an innate immune regulatory pathways (Childs et al., 2007; Childs et al., 2009) or by targeting STAT1 protein degradation at later stages (Huang et al., 2003). The ability of PA-0725 to replicate well, disseminate in multiple tissues yet still induce IFN β expression suggests that this virus might antagonize type I IFN responses by blocking the downstream signaling molecules. Because the virus infection phenotypes in chickens observed in this study have some phylogenetic pattern, the involvement of the V protein as a determinant of GVI-PMV1 viruses to productively infect and spread in chickens warrant further attention.

Our finding that phylogenetic subgroups of viruses have different phenotypes emphasizes the importance of understanding virus diversification and phylogenetic affiliation in newly emerged or introduced virus populations. Considering the large genome of PMV1 (15 kb), the overall genetic divergence among these GVI-PMV1 isolates is low ($>94\%$ similarity in nucleotide and amino acid sequence). However, small changes in a virus genome sequence can have large effects on virus phenotype in different host populations (Dortmans et al., 2011). None of the 10 viruses evaluated had mutations at sites corresponding to those reported by Dortmans et al. (2011). On the other hand, our data highlight the 77th and 92th codons in P and V genes, which are positively selected and are predicted sites of serine phosphorylation. Interestingly, the virus subgroups represented in our study differ in both the presence of a phosphorylation site and the potential for these sites to be phosphorylated. Phosphorylation sites within the P protein are important for transcription and replication of other paramyxoviruses (Sun et al., 2011) but no study has been done to date on GVI-PMV1.

Materials and methods

Virus strains, sequencing, phylogenetic and evolutionary analyses

A total of 61 GVI-PMV1 isolates from sick pigeons and chickens were recovered as described (Chong et al., 2013). Viral RNA and cDNA were prepared as described (Chong et al., 2013). The complete P and HN genes of the viruses were sequenced from two separate PCR products (primer information in Table S1). Among them, 10 pigeon-derived viral isolates were further selected and the complete viral genomes were amplified by PCR of overlapping 1 kb to 5.5 kb fragments (excluding the 5′ and 3′ termini), purified using QIAquick Gel extraction kit (Qiagen), and sequenced. The 5′ and 3′- termini were determined using the rapid amplification of cDNA ends (RACE) protocol (Li et al., 2005; Tillett et al., 2000). The GenBank accession numbers and sequence information at Table S3.

Alignments were generated for all PMV1 genomes available in GenBank in July, 2012 and the new sequences generated in this study using Muscle (Edgar, 2004). There were no significant signals of recombination detected by RDP3 (Martin et al., 2005) in these new sequences. A maximum likelihood (ML) phylogenetic tree based on the full length genomes was constructed separately by PhyML v3 program (Guindon et al., 2010). Selection analysis was done using codon-based models and maximum likelihood methods implemented in PAML (Yang, 1997) and the Datamonkey webserver (Pond and Frost, 2005). The potential phosphorylation sites at serine (S), threonine (T) and tyrosine (Y) residues in P and predicted-V protein sequences were estimated using the neural network-based method in NetPhos 2.0 Server 0.5 prediction threshold [http://www.cbs.dtu.dk/services/NetPhos/].

Sample preparation

The 10 selected GVI-PMV1 field isolates were used in the experiments. GFP-labeled LaSota vaccine strain was obtained from Dr. Siba Samal. The viruses were inoculated in 10-day old specific pathogen free (SPF) embryonated chicken eggs and propagated for three days. Allantoic fluids were harvested, and the viruses were purified and concentrated using ultracentrifugation on a 20% sucrose cushion (McGinnes et al., 2006). Purified viruses were titred using 50% tissue culture infective dose ($TCID_{50}$) assay as previously described (LaBarre and Lowy, 2001) and stored at $-80\,^{\circ}C$ until use. Purified non-infected allantoic fluid was used as a negative control for all infection experiments.

GVI-PMV1 infected chicken embryos survival assay

SPF fertilized White Leghorn chicken eggs were obtained from a local producer. The eggs were incubated in a rotary incubator at $37\,^{\circ}C$ at $50-60\%$ relative humidity. GVI-PMV1 isolates (100 μl at concentrations of $2-3\times10^2$ $TCID_{50}$) were inoculated into 10-day old chicken embryos *via* allantoic fluid as described previously (LaBarre and Lowy, 2001). Ten eggs per virus group were infected and the survival of the embryos was observed by candling and recorded three times daily for up to seven days. Death of embryos within 48 h post-inoculation (hpi) was considered to be due to non-infection related causes such as trauma and those embryos were excluded from the analysis.

GVI-PMV1 systemic infections in 18-day old chicken embryos

18-day old SPF chicken embryos were used to estimate tissue tropism and systemic infection ability of each isolate. Chicken embryos (4–7 eggs/virus group from two independent experiments) were infected *via* amniotic fluid (which is similar to commercial *in ovo* vaccination) with 100 μl inoculum containing 1×10^5 $TCID_{50}$ of virus/egg. Previous studies showed that infection was 99.5% successful *via* the amniotic fluid in 18.5 days old embryos (Wakenell et al., 2002). The amniotic fluid route of infection allows inoculum to be imbibed (swallowed) and breathed into the respiratory tract by the embryo (Williams, 2007). Lung, liver and spleen were collected at 48 hpi to allow sufficient time for at least one virus generation and dissemination into other tissues. All tissue specimens were placed into RNAlater (Ambion) immediately and incubated at $4\,^{\circ}C$ overnight. The RNAlater solutions were removed prior to storage at $-80\,^{\circ}C$. Total RNA were extracted and reverse transcribed using $oligo(dT)_{20}$ primer (Invitrogen) with the AffinityScript™ Multiple Temperature Reverse Transcriptase Kit (Stratagene) at $50\,^{\circ}C$ for 1 h and 30 min followed by heat inactivation at $65\,^{\circ}C$ for 15 min. The viral HN gene transcripts were quantified using quantitative real-time PCR (qRT-PCR) and $\log_{10}$-transformed for statistical analysis (see description below).

Primary chicken lung epithelial cells preparation

Lungs were collected from 19-day old SPF embryonated chicken eggs, washed with PBS twice and cut into small pieces followed by incubation with 1.8 U/ml DispaseI (Roche) at $37\,^{\circ}C$ for

1 h 30 min. During the last 5 min of incubation, 1 mg/ml of collagenase I (Sigma) was added. The tissue suspension was passed through nylon mesh to remove debris, and fetal bovine serum (FBS, Hyclone) was added to stop the digestion. Cells were pelleted at 800 × relative centrifugal force (RCF) for 5 min, and re-suspended in DMEM/F12 medium containing 10% FBS, 5% chicken serum (Invitrogen), 1% nonessential amino acids (Invitrogen), 1% penicillin/streptomycin (Invitrogen) and 0.05 mM β-mercaptoethanol (Sigma). The re-suspended cells were plated on fibronectin (Sigma) pre-coated flasks for 15 min to remove fibroblast cells. The cell supernatants (which contain mainly epithelial cells) were collected, counted and seeded at 2.5×10^5 cells per well in fibronectin pre-coated 12-well tissue culture plate. Lung epithelial cells were incubated overnight at 37 °C until 90% confluent based on epithelial-cadherin staining.

GVI-PMV1 infection in chicken primary lung epithelial cells

Lung epithelial cells were inoculated with GVI-PMV1 viruses, GFP-labeled LaSota, and PBS-sham control at multiplicities of infection (MOI) of 0.7 and allowed to absorb for 45 min. The supernatants were removed and replaced with 1 ml of fresh medium to synchronize the infection as 0 h post-infection. At 8 h intervals starting from 12 to 36 h post-infection, 200 μl cell-free supernatants were collected with media replacement to determine infectious virus titer using standard $TCID_{50}$ assay and cell-free viral RNA production by qRT-PCR (see below). Both total viral RNA and infectious particle numbers were log_{10}-transformed for statistical analysis.

Total cell free virus RNA enumeration by qRT-PCR

Viral RNA from supernatants of infected epithelial cells was extracted using the QIAamp Viral RNA extraction kit (Qiagen) and reverse transcribed into cDNA using strain-specific GVI-PMV1 oligonucleotide (refer to Table S1) following the protocol described above. qRT-PCR reactions were set up in duplicate in 96-well plates and amplifications were performed using B-R SYBR Green SuperMix from iQ™ (Quanta Biosciences) on the iCycler real time PCR system (IQ5; Biorad, Hercules, CA). The dissociation curve with melting temperatures was performed for quality check of the specificity of amplification products. Standards consisted of 10-fold dilutions of known concentrations of plasmids carrying the PCR fragments of interest. Cloning of standards was done using the StrataClone PCR cloning kit (Stratagene). The detailed PCR conditions and primers sequences are presented in Table S1. The viral absolute copy numbers were determined from the standard curve.

Chicken interferon beta production

The *in vitro* experiments were performed using the virus infection protocol on primary chicken epithelial lung cells as mentioned above with four independent time effects. Infected cells were harvested at 6, 10, 14 and 16 hpi. Total RNA was extracted using Trizol following manufacturer's protocols (Invitrogen). cDNA was made using oligo$(dT)_{20}$ primer (Invitrogen) as described above. IFN β transcript was measured by qRT-PCR and standardized to the production of β-actin (a host housekeeping gene). Detailed qRT-PCR conditions and reactions are shown in Table S2.

Statistical Analyses

All the statistical analyses were conducted using in house packages written in the R statistical language (Ihaka and Gentleman, 1996). The chicken embryos survival data were plotted as Kaplan – Meier curves and statistically analyzed by log rank test using Cox proportional hazards regression model (Andersen and Gill, 1982; Kalbfleisch and Prentice, 1980) from the *survival* and *KMsurv* packages implemented in R language. Factorial Analysis of Variance (ANOVA) was used to test the effects of virus subgroups and tissue types, and their interactions on the total viral transcript production *in ovo* at 48 hpi. Tukey post-hoc tests for pair-wise comparisons were done. The cell-free viral RNA produced by different viruses from *in vitro* lung epithelial cell infection were regressed on time (hpi) [treated as continuous covariate] and the regression slopes between viruses were compared to assess different growth patterns between these viruses by means of analysis of covariance (ANCOVA). Factorial Analysis of Variance (ANOVA) was used to test virus and time (independent experiment) effects, and their interactions on the total IFN β transcripts productions. Two-sample *t*-tests were done for mean comparison between virus and PBS-Sham control alone when necessary.

Multivariate approaches were used to study the association between genotype and phenotype of GVI-PMV1. Multivariate Analysis of Variance (MANOVA) were performed with Pillai's trace test (Gnanadesikan, 1997; Seber, 2004) to inform of effects of four virus subgroups (based on 10 virus types) on 12 phenotype response variables (based on *in vitro* experiments) and four phenotype response variables (based on *in ovo* experiments) separately using the *manova* function from the stats package of the R language. Since these phenotype parameters were measured in different units, the data was pre-processed by re-scaling the variables to have unit variance (mean 0 and variance 1) before the analysis was done. Principal component analysis (PCA) was performed to extract directions between the linear combinations of the phenotype variables under study and used as visualization tool of high-dimensional data to identify patterns or natural groupings. The analysis was performed using *prcomp* function from the stat package of the R language. The phenotype and genotype associations were further studied using linear discriminant analysis (LDA) by analyzing the virus subgroups (A – D – see Fig. 1B) as a function of the phenotype parameters. The phenotype parameters were standardized to have mean 0 and within groups variance of 1. This allows us to identify linear combinations of phenotype response parameters that best discriminate among the virus subgroups in a multi-dimensional data cloud. The analysis was done using *lda* function from the *MASS* package and bi-plots were drawn using *s.class* and *s.arrow* functions implemented in *ade4* package of the R language and following methods by Roy et al. (2009).

Acknowledgments

We thank Ivan Simeonov for help with survival analysis. We acknowledge technical contributions from Brian Huylebroeck and Gina Riggio. We thank the personnel in Animal Diagnostic Laboratory from The Pennsylvania State University for providing data on some of the PMV1 sequences used in this study and to the Penn State Genomics Core Facility – University Park, PA for sequencing. YLC is supported by the Malaysian Academic Training Scheme for Institutions of Higher Education Scholarship. This work was partially supported by United States Department of Agriculture Grant 2009-35204-20082, and by the RAPIDD program of the Science and Technology Directorate, U.S. Department of Homeland Security, and the Fogarty International Center, NIH, United States.

Appendix A. Supporting information

Supplementary data associated with this article can be found in the online version at http://dx.doi.org/10.1016/j.virol.2014.06.007.

References

Abolnik, C., Gerdes, G., kITCHING, J., Swanepoel, S., Romito, M., Bisschop, S., 2008. Characterization of pigeon paramyxoviruses (Newcastle disease virus) isolated in South Africa from 2001 to 2006. Onderstepoort J. Vet. Res. 75, 147–152.

Andersen, P., Gill, R., 1982. Cox's regression model for counting processes, a large sample study. Ann. Stat. 10, 1100–1120.

Barber, M.R.W., Aldridge, J.R., Webster, R.G., Magor, K.E., 2010. Association of RIG-I with innate immunity of ducks to influenza. Proc. Nat. Acad. Sci. U. S. A. 107, 5913–5918.

Childs, K., Stock, N., Ross, C., Andrejeva, J., Hilton, L., Skinner, M., Randall, R., Goodbourn, S., 2007. MDA-5, but not RIG-I, is a common target for paramyxovirus V proteins. Virology 359, 190–200.

Childs, K.S., Andrejeva, J., Randall, R.E., Goodbourn, S., 2009. Mechanism of mda-5 Inhibition by Paramyxovirus V Proteins. J. Virol. 83, 1465–1473.

Chong, Y.L., Lam, T.T.-Y., Kim, O., Lu, H., Dunn, P., Poss, M., 2013. Successful establishment and global dispersal of genotype VI avian paramyxovirus serotype 1 after cross species transmission. Infect. Genet. Evol. 17, 260–268.

Chong, Y.L., Padhi, A., Hudson, P.J., Poss, M., 2010. The effect of vaccination on the evolution and population dynamics of avian paramyxovirus-1. PLoS Pathog. 6, e1000872.

Dortmans, J.C.F.M., Rottier, P.J.M., Koch, G., Peeters, B.P.H., 2010. The viral replication complex is associated with the virulence of newcastle disease virus. J. Virol. 84, 10113–10120.

Dortmans, J.C.F.M., Rottier, P.J.M., Koch, G., Peeters, B.P.H., 2011. Passaging of a Newcastle disease virus pigeon variant in chickens results in selection of viruses with mutations in the polymerase complex enhancing virus replication and virulence. J. Gen. Virol. 92, 336–345.

Edgar, R.C., 2004. MUSCLE: multiple sequence alignment with high accuracy and high throughput. Nucleic Acids Res. 32, 1792–1797.

Fuller, C.M., Collins, M.S., Easton, A.J., Alexander, D.J., 2007. Partial characterisation of five cloned viruses differing in pathogenicity, obtained from a single isolate of pigeon paramyxovirus type 1 (PPMV-1) following passage in fowls' eggs. Arch. Virol. 152, 1575–1582.

Gelb Jr., J., Fries, P.A., Peterson, F.S., 1987. Pathogenicity and cross-protection of pigeon paramyxovirus-1 and Newcastle disease virus in young chickens. Avian Dis. 31, 601–606.

Gnanadesikan, R., 1997. Methods for Statistical Data Analysis of Multivariate Observations. Wiley, New York.

Goodbourn, S., Didcock, L., Randall, R.E., 2000. Interferons: cell signalling, immune modulation, antiviral response and virus countermeasures. J. Gen. Virol. 81, 2341–2364.

Guindon, S., Dufayard, J.-F., Lefort, V., Anisimova, M., Hordijk, W., Gascuel, O., 2010. New algorithms and methods to estimate maximum-likelihood phylogenies: assessing the performance of PhyML 3.0. Syst. Biol. 59, 307–321.

Hassan, W., Khair, S.A., Mochotlhoane, B., Abolnik, C., 2010. Newcastle disease outbreaks in the Sudan from 2003 to 2006 were caused by viruses of genotype 5d. Virus Genes 40, 106–110.

Huang, Z., Krishnamurthy, S., Panda, A., Samal, S.K., 2003. Newcastle disease virus V protein is associated with viral pathogenesis and functions as an alpha interferon antagonist. J. Virol. 77, 8676–8685.

Ihaka, R., Gentleman, R., 1996. R: a language for data analysis and graphics. J. Comput. Graphical Stat. 5, 299–314.

Kalbfleisch, D., Prentice, R.L., 1980. The Statistical Analysis of Failure Time Data. Wiley, New York.

Kim, L.M., King, D.J., Guzman, H., Tesh, R.B., Travassos da Rosa, A.P., Bueno Jr., R., Dennett, J.A., Afonso, C.L., 2008. Biological and phylogenetic characterization of pigeon paramyxovirus serotype 1 circulating in wild North American pigeons and doves. J. Clin. Microbiol. 46, 3303–3310.

King, D.J., 1996. Avian paramyxovirus type 1 from pigeons: isolate characterization and pathogenicity after chicken or embryo passage of selected isolates. Avian Dis. 40, 707–714.

Kommers, G.D., King, D.J., Seal, B.S., Brown, C.C., 2001. Virulence of pigeon-origin Newcastle disease virus isolates for domestic chickens. Avian Dis. 45, 906–921.

LaBarre, D.D., Lowy, R.J., 2001. Improvements in methods for calculating virus titer estimates from TCID50 and plaque assays. J. Virol. Methods 96, 107–126.

Li, Z., Yu, M., Zhang, H., Wang, H.Y., Wang, L.F., 2005. Improved rapid amplification of cDNA ends (RACE) for mapping both the 5′ and 3′ terminal sequences of paramyxovirus genomes. J. Virol. Methods 130, 154–156.

Liu, H., Wang, Z., Son, C., Wang, Y., Yu, B., Zheng, D., Sun, C., Wu, Y., 2006. Characterization of pigeon-origin Newcastle disease virus isolated in China. Avian Dis. 50, 636–640.

Martin, D.P., Williamson, C., Posada, D., 2005. RDP2: recombination detection and analysis from sequence alignments. Bioinformatics 21, 260–262.

Mase, M., Imai, K., Sanada, Y., Sanada, N., Yuasa, N., Imada, T., Tsukamoto, K., Yamaguchi, S., 2002. Phylogenetic analysis of Newcastle disease virus genotypes isolated in Japan. J. Clin. Microbiol. 40, 3826–3830.

McGinnes, L., Pantua, H., Reitter, J., Morrison, T., 2006. Newcastle disease virus: propagation, quantification, and storage. In: Coico, R., Kowalik, T., Quarles, J., Stevenson, B., Taylor, R. (Eds.), Current Protocols in Microbiology. John Wiley & Sons, Inc., New York.

Mebatsion, T., Verstegen, S., De Vaan, L.T., Romer-Oberdorfer, A., Schrier, C.C., 2001. A recombinant newcastle disease virus with low-level V protein expression is immunogenic and lacks pathogenicity for chicken embryos. J. Virol. 75, 420–428.

Meulemans, G., van den Berg, T.P., Decaesstecker, M., Boschmans, M., 2002. Evolution of pigeon Newcastle disease virus strains. Avian Pathol. 31, 515–519.

Park, M.S., Garcia-Sastre, A., Cros, J.F., Basler, C.F., Palese, P., 2003. Newcastle disease virus V protein is a determinant of host range restriction. J. Virol. 77, 9522–9532.

Pearson, J.E., Senne, D.A., Alexander, D.J., Taylor, W.D., Peterson, L.A., Russell, P.H., 1987. Characterization of newcastle disease virus (Avian Paramyxovirus-1) isolated from pigeons. Avian Dis. 31, 105–111.

Pedersen, J.C., Senne, D.A., Woolcock, P.R., Kinde, H., King, D.J., Wise, M.G., Panigrahy, B., Seal, B.S., 2004. Phylogenetic relationships among virulent Newcastle disease virus isolates from the 2002-2003 outbreak in California and other recent outbreaks in North America. J. Clin. Microbiol. 42, 2329–2334.

Pond, S.L., Frost, S.D., 2005. Datamonkey: rapid detection of selective pressure on individual sites of codon alignments. Bioinformatics 21, 2531–2533.

Poole, E., He, B., Lamb, R.A., Randall, R.E., Goodbourn, S., 2002. The V proteins of simian virus 5 and other paramyxoviruses inhibit induction of interferon-β. Virology 303, 33–46.

Roy, S., Lavine, J., Chiaromonte, F., Terwee, J., VandeWoude, S., Bjornstad, O., Poss, M., 2009. Multivariate statistical analyses demonstrate unique host immune responses to single and dual lentiviral infection. PLoS ONE 4, e7359.

Seber, G., 2004. Multivariate Obeservations. Wiley, New York.

Steward, M., Vipond, I.B., Millar, N.S., Emmerson, P.T., 1993. RNA editing in Newcastle disease virus. J. Gen. Virol. 74 (Pt 12), 2539–2547.

Sun, D., Luthra, P., Xu, P., Yoon, H., He, B., 2011. Identification of a phosphorylation site within the P protein important for mRNA transcription and growth of parainfluenza virus 5. J. Virol. 85, 8376–8385.

Tillett, D., Burns, B.P., Neilan, B.A., 2000. Optimized rapid amplification of cDNA ends (RACE) for mapping bacterial mRNA transcripts. BioTechniques 28, 448–456.

Toro, H., Hoerr, F.J., Farmer, K., Dykstra, C.C., Roberts, S.R., Perdue, M., 2005. Pigeon paramyxovirus: association with common avian pathogens in chickens and serologic survey in wild birds. Avian Dis. 49, 92–98.

Ujvari, D., Wehmann, E., Kaleta, E.F., Werner, O., Savic, V., Nagy, E., Czifra, G., Lomniczi, B., 2003. Phylogenetic analysis reveals extensive evolution of avian paramyxovirus type 1 strains of pigeons (Columba livia) and suggests multiple species transmission. Virus Res. 96, 63–73.

van Boxel-Dezaire, A.H.H., Rani, M.R.S., Stark, G.R., 2006. Complex modulation of cell type-specific signaling in response to Type I interferons. Immunity 25, 361–372.

Wakamatsu, N., King, D.J., Seal, B.S., Peeters, B.P.H., Brown, C.C., 2006. The effect on pathogenesis of newcastle disease virus LaSota strain from a mutation of the fusion cleavage site to a virulent sequence (Efecto en la patogenia de la cepa LaSota del virus de la enfermedad de Newcastle con una mutación en el sitio de corte de la proteína de fusión hacia una secuencia virulenta). Avian Dis. 50, 483–488.

Wakenell, P.S., Bryan, T., Schaeffer, J., Avakian, A., Williams, C., Whitfill, C., 2002. Effect of in ovo vaccine delivery route on herpesvirus of turkeys/SB-1 efficacy and viremia. Avian Dis. 46, 274–280.

Wesoly, J., Szweykowska-Kulinska, Z., Bluyssen, H.A., 2007. STAT activation and differential complex formation dictate selectivity of interferon responses. Acta Biochim. Pol. 54, 27–38.

Williams, C.J., 2007. In ovo vaccination for disease prevention. Int. Poult. Prod. 15, 7–9.

Yang, Z., 1997. PAML: a program package for phylogenetic analysis by maximum likelihood. Bioinformatics 13, 555–556.